Differentiation of Flavonoid Glycoside Isomers by Using Metal Complexation and Electrospray Ionization Mass Spectrometry

Michael Pikulski and Jennifer S. Brodbelt

Department of Chemistry and Biochemistry, The University of Texas at Austin, Austin, Texas, USA

The elucidation of flavonoid isomers is accomplished by electrospray ionization tandem mass spectrometry (ESI-MS/MS) via formation and collisional activated dissociation (CAD) of metal/flavonoid complexes containing an auxiliary ligand. Addition of a metal salt and a suitable neutral auxiliary ligand to flavonoids in solution results in the formation of [M(II) (flavonoid-H) ligand]$^+$ complexes by ESI which, upon collisional activated dissociation, often result in more distinctive fragmentation patterns than observed for conventional protonated or deprotonated flavonoids. Previously, 2,2'-bipyridine was used as an auxiliary ligand, and now we compare and explore the use of alternative pyridyl ligands, including 4,7-diphenyl-1,10-phenanthroline. Using this technique, three groups of flavonoid glycoside isomers are differentiated, including glycosides of apigenin, quercetin, and luteolin.   (J Am Soc Mass Spectrom 2003, 14, 1437–1453) © 2003 American Society for Mass Spectrometry

Flavonoids are polyphenolic phytochemicals which occur in edible fruits and vegetables. They have been reported to act as antioxidants [1], antimicrobials [2], free radical scavengers [1], metal chelators [1], and anti-viral and anti-bacterial agents [3]. Since they are a ubiquitous part of the human diet, their effect on human health is of interest. Flavonoids are known to have medicinal and chemopreventive activities in humans [4–7]. For example, a diet rich in flavonoids has shown to have an inverse relationship with heart disease [8–10].

There is a basic structure which is common to all flavonoids; however, there is a great diversity of flavonoids due to different hydroxylation and glycosylation positions. Most flavonoids exist as glycosides in plant sources, and many only differ by the nature of the aglycone, and/or by the glycosylation site, the sequence, and the interglycosidic linkages of the glycan portion. The biological activities of flavonoids are affected by these subtle structural differences [11]. Therefore, there is a critical need for the development of analytical methods to elucidate structurally similar compounds.

A number of mass spectrometric techniques have been used to study the structures of flavonoids [12]. Electron ionization (EI) has been used to evaluate the fragmentation pathways of some aglycones [13] and for limited structural studies of glycosides. However, der-

ivatization was required to make the flavonoids sufficiently volatile for EI and in some cases did not result in meaningful fragmentation patterns [14–17]. Fast atom bombardment (FAB) and liquid secondary ion mass spectrometry (LSIMS) have been used extensively [18–36]. In addition, thermospray [37–39] and atmospheric pressure chemical ionization (APCI) [40, 41] have been used for several applications involving the analysis of flavonoids. Most recent, electrospray ionization (ESI) has become a popular choice [40–49]. For example, the positive ESI mode was used to identify and quantitate flavonoids in soya flours and baby foods [43], and in hops and beer [48]. Also, the negative ESI mode was used to identify and quantitate flavonoids in tea extracts [44] and plants such as *Passiflora incarnata* [47].

Tandem mass spectrometry has been used to elucidate many of these compounds [23, 24, 31–36, 44, 47, 50–52]. For example, CAD of deprotonated flavonoid glycosides commonly results in loss of the sugars (formation of Y_0^- and Y_1^- ions). CAD of deprotonated flavonoid-O-glycosides allows distinction of rutinosides (1 → 6 disaccharides) from neohesperidosides (1 → 2 disaccharides) based on the greater abundance of the Y_1^- ions for the neohesperidosides compared to the rutinosides [50]. However, unique fragment ions were not observed for each isomer in all cases, so some identifications were based on differences in abundances of fragment ions of the same *m/z* values. In addition, CAD of protonated flavonoid-C-glycosides allowed the differentiation between 6-C and 8-C glycosides [51]. However, the isomeric distinctions generally relied on the relative abundances of common product ions in the MS/MS spectra for some compounds, and diagnostic

product ions were only observed in the MS/MS/MS spectra. Hvattum et al. used CAD to evaluate the formation of radical fragment ions from deprotonated flavonoid glycosides by loss of neutral sugar radicals [52]. The radical fragmentation processes were related to the number of hydroxyl substituents on the B ring of the flavonoid, in addition to the type and position of the sugar substituent. It was surmised that the radical loss of the 3–O-sugar substituent was enhanced by the presence of multiple hydroxyl groups on the B ring due to the electron-donating properties of the hydroxyl groups, thus weakening the glycosidic bonds.

Due to their acidic functional groups, protonation of flavonoid glycosides is inefficient, often resulting in weak positive ESI mass spectra. In some cases, the fragmentation patterns of protonated flavonoids do not differentiate similar compounds or isomers. Although deprotonation results in more intense mass spectra in the negative ESI mode, the fragmentation patterns again frequently do not differentiate similar compounds or isomers. Metal complexation is an alternative ionization mode which has been explored in the Brodbelt group in the past [53–58]. It has been observed that metal complexation can both increase ion intensity and alter fragmentation pathways, resulting in many more structurally distinctive fragment ions. Dramatic increases in intensities of some flavonoids [56] have been observed with the use of copper, nickel, or cobalt, along with 2,2′-bipyridine or 1,10-phenanthroline as an auxiliary ligand. In this study, we show differentiation of three series of flavonoid glycosides with the use of 2,2′-bipyridine (bpy) and 4,7-diphenyl-1,10-phenanthroline (dpphen), a new auxiliary ligand. Although some of these compounds have been differentiated in the positive ion mode based on differences in the relative intensities of specific fragment ions [50, 51] and in the negative ion mode based on low intensity fragment ions formed upon CAD [51], in this work we are able to differentiate isomers via more intense, distinctive ions in the CAD spectra.

Two classes of flavonoids, flavones and flavonols, are considered in this study. In the present report, we extend and expand the use of metal complexation for differentiation within these two classes of flavonoids. We accomplish differentiation of glycosides of apigenins, commonly found in olive oil [59], orange juice [60], celery [61], and garlic [62] (Figure 1, Group I); in addition to glycosides of kaempferol, commonly found in lettuce [64], green beans [65], and grapes [66], glycosides of quercetin, commonly found in onions [63], kale [64], lettuce [64], and green beans [65] and glycosides of luteolin, commonly found in broccoli [62], carrots [62], and celery (Figure 1, Group II) [62].

Experimental

Experiments were performed with a Thermoquest LCQ Duo quadruple ion trap mass spectrometer equipped with an electrospray ionization source. The flow rate of

the solutions was 5 μL min^{-1}. The lens and octapole voltages, sheath gas flow rate and capillary voltage were optimized for maximum intensity of the ion of interest. The capillary temperature was 200 °C. The interface pressure, measured with the convectron gauge at the skimmer cone, was normally 0.9 torr. The pressure in the ion trap with helium added was nominally 1.9×10^{-5} torr, measured by the ionization gauge. The spectra were acquired with ion injection times of 5 ms and an average of 10 microscans.

In the negative ESI mode, the ion corresponding to [L-H]$^{-}$ was optimized, where L is the flavonoid. In the positive ESI mode, when solutions of flavonoid/metal/auxiliary ligand were used, the ion corresponding to [M(II) (L-H) A]$^{+}$ was optimized, where M is the metal and A is the auxiliary ligand. During MS/MS experiments, these parent ions were isolated and the CAD voltage was adjusted so that the parent ion intensity decreased to 20% of the base peak.

Stock solutions of 4.0×10^{-4} M metal salt/methanol and 4.0×10^{-4} M auxiliary ligand/methanol were used to create the analytical solutions. Solutions containing a flavonoid, a metal salt, and an auxiliary ligand were ~1:1:1 at 1.0×10^{-5} M. The analytical solutions used for the negative ESI experiments were 1.0×10^{-5} M flavonoid in methanol.

The flavonoids apigenin, vitexin, apigenin-7-glucoside, isorhoifolin, rhoifolin, isovitexin, quercetin, luteolin, quercitrin, kaempferol-3-glucoside, luteolin-4′-glucoside, luteolin-7-glucoside and orientin were purchased from Indofine (Somerville, NJ). 2,2′-Bipyridine, 4,7-diphenyl-1,10-phenanthroline, 1,10-phenanthroline, 2,2′:6′,2″-terpyridine, 4,4′-dimethyl-2,2′-bipyridine, CoBr$_2$, NiBr$_2$, and CuBr$_2$ were purchased from Aldrich (Milwaukee, WI). The HPLC grade methanol was purchased from EM Science (Gibbstown, NJ). All materials were used without further purification.

The nomenclature for glycoconjugates proposed by Domon and Costello [67] is used to describe the fragmentation pathways for O-glycosides. Fragments from a terminal sugar unit are labeled using $^{g,h}A_i$, B_i and C_i, where i is the number of the bond broken, counting from the terminal sugar beginning with 1, and g and h are the cross-ring cleavages of the sugar. Fragments which include the aglycone are labeled $^{k,l}X_j$, Y_j, and Z_j, where j is the number of the bond broken, counting from the aglycone beginning with 0, and k and l are the cross-ring cleavages of the sugar.

Results and Discussion

Negative Ion Mode

Since the negative ESI mode has been so widely used for mass spectrometric analysis of flavonoids, we have compared the relative ionization efficiencies and diagnostic utility of the CAD spectra for deprotonated flavonoids to those obtained for the metal complexes in the present study. The spectra collected in the negative
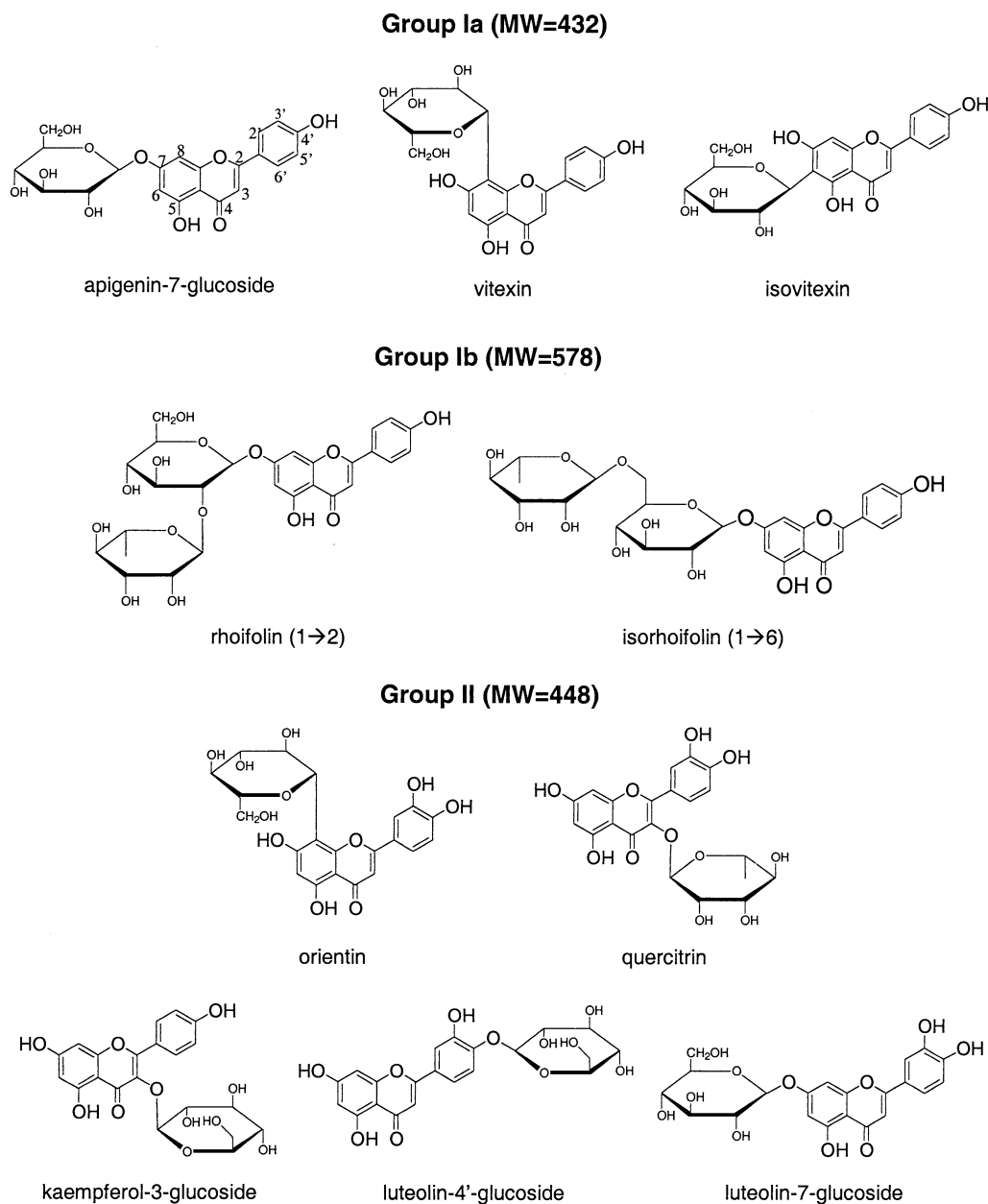
Group Ia (MW=432)

apigenin-7-glucoside   vitexin   isovitexin

Group Ib (MW=578)

rhoifolin (1→2)   isorhoifolin (1→6)

Group II (MW=448)

orientin   quercitrin

kaempferol-3-glucoside   luteolin-4'-glucoside   luteolin-7-glucoside

Figure 1. Structures of flavonoids studied, with molecular weights in parentheses.

ion mode were clean with intense ions due to the efficiency of deprotonation of the flavonoids. The spectra were dominated by $[L-H]^-$ ions, the ion selected for the CAD studies. Also observed were $[L\ (L-H)]^-$ ions; dissociation of these dimer species yielded $[L-H]^-$ ions. The following sections describe the CAD results for the deprotonated flavonoids of the three sets of isomers in order to establish benchmarks for the degree of differentiation.

Group Ia differentiation: Apigenin-7-glucoside, Vitexin, and Isovitexin (MW 432). The CAD mass spectra of the Group Ia flavonoids are shown in Figure 2, and the MS^n data for the Group I flavonoids in the negative ESI
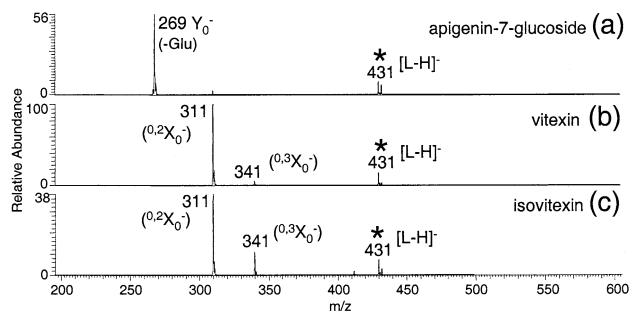

Figure 2. CAD spectra for deprotonated flavonoids from Group Ia. The parent ions are labeled with asterisks.

Table 1. MS^n Spectra of deprotonated Group I flavonoids

		MS/MS[a]			MS/MS/MS[a]		
	m/z	*m/z*	Loss	%	*m/z*	Loss	%
Apigenin-7-glucoside	431	269	162	100	225	44	100
					197	72	36
					120	149	28
		311	120	6			
Vitexin	431	311	120	100	283	28	100
		341	90	6			
Isovitexin	431	311	120	100	283	28	100
		341	90	28	323	18	100
					269	72	8
					311	30	6
Rhoifolin	577	269	308	100	225	44	100
		413	164	4			
		311	266	3			
		431	146	3			
		457	120	2			
		371	206	2			
Isorhoifolin	577	269	308	100	225	44	100

[a]MS/MS and MS/MS/MS data correspond to their parent ions (labeled *m/z*) on the left. The standard deviations of the fragment ion intensities are typically ±5%.

mode is summarized in Table 1. Upon CAD of the deprotonated flavonoids, the O-bonded glucoside, apigenin-7-glucoside, is easily differentiated from the C-bonded isomers, isovitexin and vitexin, because deprotonated apigenin-7-glucoside dissociates primarily by loss of the glucose residue (Glu) (−162 Da) resulting in the Y_0^- ion at *m/z* 269 (Figure 2a). Likewise, both of the C-bonded glucosides, vitexin and isovitexin, are easily differentiated from apigenin-7-glucoside because the deprotonated species dissociate by losses of 120 and 90 Da due to cross-ring sugar cleavages (corresponding to $^{0,2}X_0^-$ and $^{0,3}X_0^-$, respectively, Figure 2b and c). Cross-ring cleavages are commonly observed in the dissociation of saccharides [67–72], and this type of process is also observed for the C-bonded glycosides [18, 23] since the typical rearrangements across the oxygen glycosidic bond do not take place. However, the CAD spectra of deprotonated vitexin and isovitexin do not have significant diagnostic ions which differentiate them from each other in the negative ESI mode, nor can the intensities of the two major fragment ions (with identical mass-to-charge values for each isomer) be used to reliably distinguish and quantify the two flavonoids in mixtures. A second stage of ion isolation and activation (i.e., MS/MS/MS) undertaken on the major fragment ion at *m/z* 311 (seen in Figure 2b and c) results exclusively in the loss of CO for both vitexin and isovitexin, so even MS^n does not sufficiently differentiate these two compounds. This lack of isomer differentiation is a good example of why other ionization modes that might create different types of precursor ions with more distinctive dissociation properties should be explored.

Group Ib differentiation: Rhoifolin and Isorhoifolin (MW 578). Both deprotonated rhoifolin and isorhoifolin dissociate primarily by loss of the disaccharide, resulting

in the Y_0^- ion at *m/z* 269 (Figure 3a and b). Although these two isomers in theory may be differentiated by the occurrence of several unique losses from deprotonated rhoifolin (formation of ions at *m/z* 311, 371, 431, and 457) [50], these ions are less than 5% relative intensity in the CAD spectra and could fall below limits of detection in more complex samples. Further fragmentation of the Y_0^- ion results in the loss of CO_2 for each isomer. Thus, CAD of deprotonated rhoifolin and isorhoifolin does not differentiate these isomers with confidence.

Group II differentiation (MW 448). The CAD mass spectra for the five deprotonated flavonoids in Group II are shown in Figure 3, and the MS^n data is summarized in Table 2. Deprotonated orientin, the C-bonded isomer, is easily differentiated from the others by the losses of 120 Da and 90 Da due to cross-ring cleavages (Figure 4a), which are observed for some of the Group Ia flavonoids. In addition, deprotonated quercitrin is distinguished from the others because of the unique loss of the terminal rhamnose residue (Rha) (−146 Da), resulting in the Y_0^- ion at *m/z* 301 (Figure 4b). The deproto-
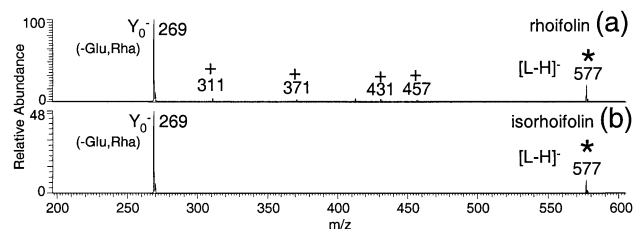

Figure 3. CAD spectra for deprotonated flavonoids from Group Ib. The parent ions are labeled with asterisks. The plus symbols represent previously identified low-intensity ions which could fall below limits of detection in more complex samples.

Table 2. MS^n Spectra of deprotonated Group II flavonoids

	m/z	MS/MS[a]			MS/MS/MS[a]		
		m/z	Loss	%	m/z	Loss	%
Orientin	447	327	120	100			
	357	90	54				
Quercitrin	447	301	146	100			
		300	147	26			
Kaempferol-3-glucoside	447	284	163	100	255	29	100
					256	28	32
					227	57	6
		285	162	53			
		327	120	14			
Luteolin-4′-glucoside	447	285	162	100	241	44	100
					199	86	82
					243	42	59
					217	68	51
					175	110	40
					242	43	27
					257	28	22
					151	134	21
					213	72	20
					218	67	18
					223	62	15
					267	18	10
Luteolin-7-glucoside	447	285	162	100	241	44	100
					199	86	77
					217	68	69
					243	42	67
					175	110	60
					213	72	26
					257	28	24
					242	43	21
					151	134	21
					267	18	17

[a]MS/MS and MS/MS/MS data correspond to their parent ions (labeled m/z) on the left. The standard deviations of the fragment ion intensities are typically ±5%.

nated flavonoids of the remaining three isomers, the O-glucosides, each dissociate by loss of their terminal Glu (−162 Da, formation of m/z 285) (Figure 4c, d, and e). In addition to the prominent loss of Glu, deproto-

Figure 4. CAD spectra for deprotonated flavonoids from Group II. The parent ions are labeled with asterisks.

nated kaempferol-3-glucoside undergoes an even more pronounced radical loss of the sugar, presumably via a homolytic bond cleavage [52] at the 3–O-glucose bond which results in the ion at m/z 284. Note that this type of process also occurs for deprotonated quercitrin (leading to the Y_0^- ion at m/z 300), although to a much lesser extent. These two isomers both have their sugars attached at the 3 position. The radical ion pathway was only observed for 3-substituted flavonoid glycosides and not for the 7-glucoside, luteolin7-glucoside, as has been reported [52]. The exact structure of the radical Y_0^- ion at m/z 284 is difficult to define because there are several possible sites of deprotonation of the flavonoids, and thus a variety of reasonable initial precursor structures and final product structures can be drawn and in which the resulting oxygen radical site can be stabilized via resonance.

The remaining two isomers, deprotonated luteolin-4′-glucoside and luteolin-7-glucoside, are not differentiated by CAD nor by MS^3 spectra. While the fragmentation of the primary fragment ion (m/z 285) is extensive in the MS^3 spectra obtained for deprotonated luteolin-4′-glucoside and luteolin-7-glucoside (see Table 2), the
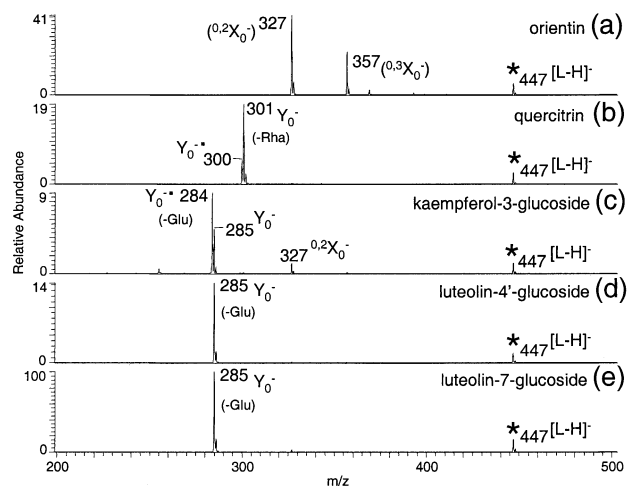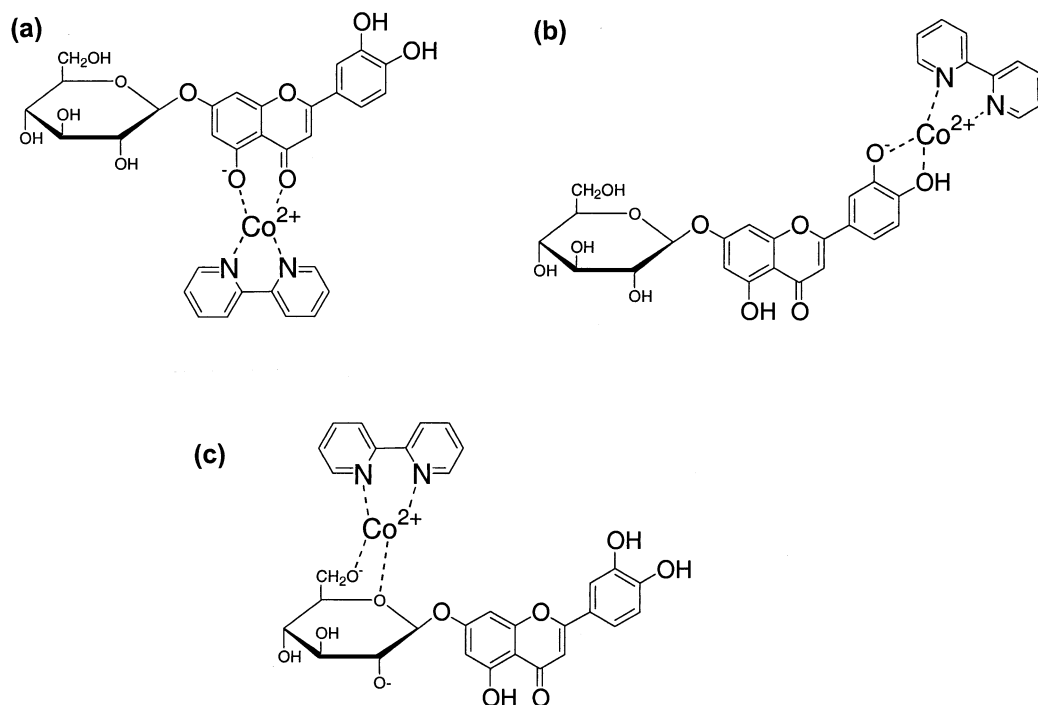
Figure 5. Proposed structures for [Co(II) (L-H) bpy]$^+$ complexes.

ions are similar and do not unequivocally distinguish these two isomers in the negative ion mode. Most of the secondary fragmentation pathways involve losses of CO, CO_2 and H_2O from the selected primary fragment ion (m/z 285). For example, both of the MS/MS/MS spectra are dominated by a loss of 44, the loss of CO_2, from m/z 285.

Metal Complexation

Due to the unsatisfactory differentiation of the flavonoid isomers based on CAD mass spectra of the deprotonated flavonoids, metal complexation was explored as an alternative way to ionize the flavonoids and create different types of parent structures. Due to our previous studies in this area [53–58], 2,2'-bipyridine was selected as the first auxiliary ligand and $CoBr_2$ was used as the metal salt. For the flavonoids, acidic sites that may be deprotonated in solution and are adjacent to a second binding site (i.e., another oxygen atom) are the likely chelation sites for the metal ions. Using luteolin-7-glucoside as an example, the metal binding site may be between the carbonyl functionality and a deprotonated hydroxyl at the 5 position (Figure 5a), or between adjacent hydroxyls on the B ring, one being deprotonated (Figure 5b), or even involve the sugar moiety (Figure 5c). The structures shown in Figure 5 are just a subset of reasonable possibilities, and the ESI process may generate a mixture of these metal complexes. Complexes of the type [M(II) (L-H) A]$^+$ where M is the metal, A is the auxiliary ligand, and L is the flavonoid, were produced for copper, cobalt, and nickel,

and all of these complexes were more intense than the deprotonated flavonoids. While the copper and nickel complexes were more intense than the cobalt complexes, the latter produced ions which enabled differentiation of the isomers upon CAD. Thus, $CoBr_2$ was used for the remainder of the study, and only the CAD spectra of the [Co(II) (flavonoid-H) 2,2'-bipyridine]$^+$ complexes were evaluated for the isomers.

Complexation with Cobalt and 2,2'-Bipyridine

Upon ESI of solutions containing one flavonoid, a cobalt salt, and 2,2'-bipyridine, ions observed in these spectra included [Co(II) (L-H) 2 × bpy]$^+$ and [Co(II) (L-H) bpy]$^+$, with the latter being about five times more intense than the former. In addition, there were minor product ions due to in-source fragmentation of the sugar for the O-bonded isomers, such as the loss of
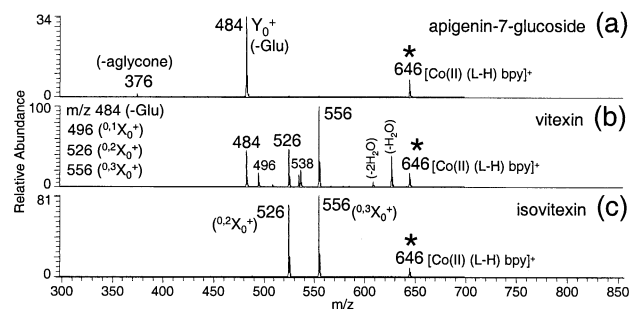

Figure 6. CAD spectra of [Co(II) (L-H) bpy]$^+$ complexes of Group Ia flavonoids. The parent ions are labeled with asterisks.
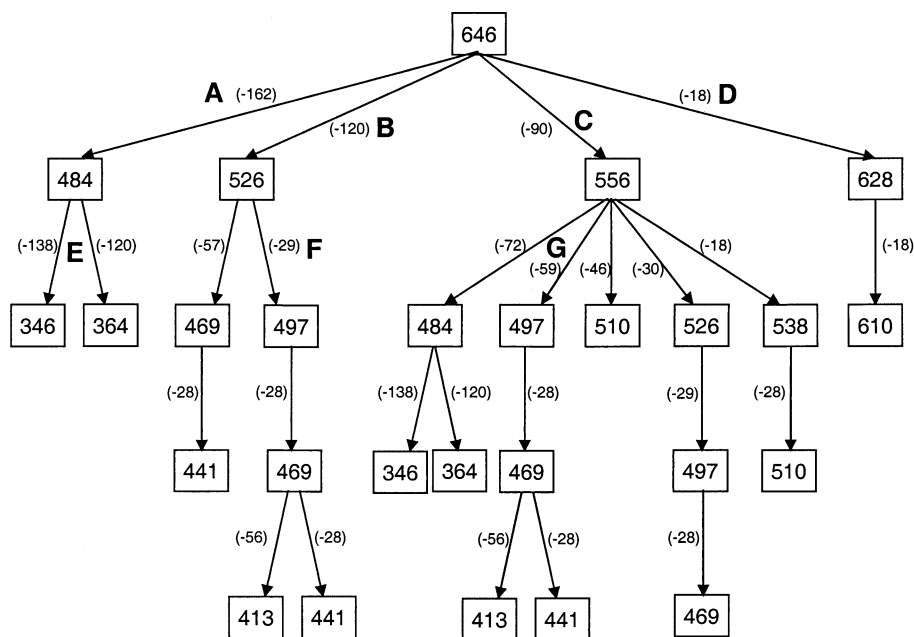
Table 3. MS^n Spectra of Group I [Co(II) (L-H) bpy]$^+$ Complexes

		MS/MS[a]			MS/MS/MS[a]		
	m/z	m/z	Loss	%	m/z	Loss	%
Apigenin-7-glucoside	646	484	162	100	364	120	100
					346	138	23
		376	270	4			
Vitexin	646	556	90	100	497	59	100
					538	18	60
					510	46	42
					526	30	19
					484	72	9
		526	120	46	497	29	100
					469	57	15
		484	162	46	364	120	100
					346	138	20
					377	107	5
					456	28	5
					254	230	3
		628	18	38	610	18	100
					568	60	20
					497	131	16
					525	103	12
					550	78	10
					592	36	9
					508	120	7
					580	48	6
		538	108				
		496	150				
		536	110				
		610	36				
Isovitexin	646	556	90	100	497	59	100
					538	18	86
					536	20	80
					498	58	61
					510	46	64
					496	60	25
					484	72	16
		526	120	90	508	18	100
					497	29	81
					498	28	81
					496	30	50
					232	294	31
					216	310	13
					469	57	11
Rhoifolin	792	484	308	100	364	120	100
					346	138	28
		646	146	24	484	162	100
					376	270	4
		376	416	10			
Isorhoifolin	792	484	308	100	364	120	100
					346	138	22
		646	146	45	484	162	100

[a]MS/MS and MS/MS/MS data correspond to their parent ions (labeled m/z) on the left. The standard deviations of the fragment ion intensities are typically ±5%.

terminal Rha or the entire disaccharide. The [Co(II) (L-H) bpy]$^+$ complexes formed were generally an order of magnitude more intense than the [L-H]$^-$ ions formed in the negative ion mode. In addition to this improvement in sensitivity, the CAD fragmentation patterns were generally richer and more distinctive than those observed for the negative ion mode.

Group Ia differentiation: Apigenin-7-glucoside, Vitexin and Isovitexin (MW 432). The CAD spectra of the [Co(II) (L-H) bpy]$^+$ complexes are illustrated in Figure 6 for the group Ia isomers and the MS^3 data is tabulated in Table 3. The CAD spectrum for the apigenin-7-glucoside complex is distinctive from the other two isomers in that there is only one major ion (Y$_0^+$complex, m/z 484)

646

A (-162)   (-120) B   (-90) C   (-18) D

484   526   556   628

(-138) E (-120)   (-57) (-29) F   (-72) G (-18)   (-18)
(-59) (-46) (-30)

346   364   469   497   484   497   510   526   538   610

(-28)   (-28)   (-138) (-120)   (-28)   (-29)   (-28)

441   469   346   364   469   497   510

(-56) (-28)   (-56) (-28)   (-28)

413   441   413   441   469

Scheme 1. CAD fragmentation pathways for $[Co(II)\ (vitexin-H)\ bpy]^{+}$ using m/z values of the fragment ions.

due to the loss of Glu (Figure 6a). In addition, there is a low intensity ion due to the loss of the aglycone moiety at m/z 376. The loss of the entire aglycone moiety from the complex means that the cobalt ion and 2,2′-bipyridine are coordinated only to the sugar moiety in the resulting product ion, suggesting that the initial structure proposed in Figure 5c may be operative or that the cobalt/2,2′-bipyridine moiety may migrate from the aglycone to the saccharide upon collisional activation of the complex. The $[Co(II)\ (L-H)\ bpy]^{+}$ complex of vitexin also undergoes the loss of the Glu upon CAD which is common for the O-glycosides but was not expected for a C-bonded glycoside. The losses of 120 and 90 Da due to cross-ring cleavages are also dominant (Figure 6b). In addition, the vitexin complex dissociates by several other pathways, including the loss of 150 Da ($^{0,1}X_0^+$), a similar neutral loss to which has been reported in the positive ion mode [23], and the loss of one or two molecules of water. While the $[Co(II)\ (L-H)\ bpy]^{+}$ complexes of vitexin also undergo two of the same cross-ring cleavages as does the vitexin isomer, resulting in losses of 90 and 120 Da (Figure 6c), the losses from Glu, 150 and 108 Da, are unique for the isovitexin complex. The latter loss of 108 Da was the same as one of the neutral losses also observed in the positive ion mode [23] and was proposed to be due to elimination of 90 Da in conjunction with water. Thus, comparison of the CAD spectra in Figure 2b and c to those seen in Figure 6b and c confirms that isovitexin and vitexin are more effectively differentiated based on the results for the metal complexes.

Due to the diverse array of fragmentation pathways for the $[Co(II)\ (L-H)\ bpy]^{+}$ complex of vitexin, this complex serves as an excellent model to illustrate the general fragmentation genealogy of the metal complexes. Scheme **1** shows the m/z values of the product ions and neutral losses based on extensive MS^n experiments, and Scheme **2** illustrates proposed structures that reasonably account for the major fragment ions. Schemes **1** and **2** refer specifically to the ions seen in Figure 6b for the vitexin complex, but many of the pathways are general ones seen for the other isomers. Path A represents the loss of the terminal sugar, which is most prevalent with the O-glucosides. This fragmentation route is followed by Path E, the loss of 2,2′-bipyridine and addition of two water molecules, resulting in the ion at m/z 364. Sometimes this pathway occurs with the addition of only one molecule of water (formation of m/z 346). Solvation of metal complexes in an ion trap has been noted previously [72–76] and is attributed to the coordinative unsaturation of the metal center which is resolved by the adduction of water molecules, present at low levels in the trap. The pathway proposed as involving loss of 2,2′-bipyridine and attachment of water molecules (Path E) was confirmed by CAD of a $[Co(II)\ (L-H)\ phen]^{+}$ complex containing cobalt with 1,10-phenanthroline (phen) instead of 2,2′-bipyridine. The appearance of the same product ions at m/z 346 and 364 confirmed that the auxiliary ligand was lost from the metal complexes upon activation, otherwise these fragment ions would be shifted upwards in m/z value by the difference between the nominal mass of 2,2′-bipyridine and 1,10-phenanthroline. Thus, Path E for the $[Co(II)\ (L-H)\ bpy]^{+}$ complex is actually the loss of 2,2′-bipyridine (156 Da) followed by the rapid adduction of one or two water molecules.

Path B depicts the cross-ring cleavage resulting in a loss of 120 Da. The resulting ion further dissociates
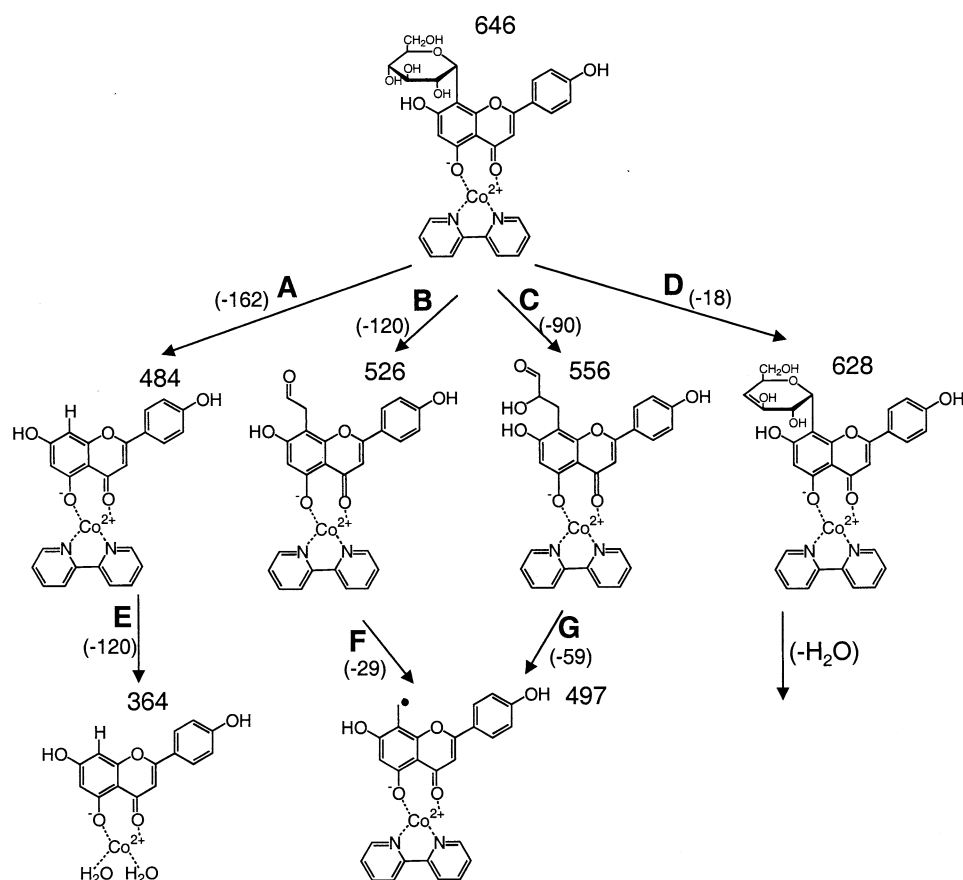
Scheme 2. CAD fragmentation pathways for [Co(II) (vitexin-H) bpy]$^+$ using proposed structures of the fragment ions.

predominantly by Path F, resulting in an interesting radical species of m/z 497 via the loss of CHO· radical. There is also a less intense secondary fragment ion at m/z 469, assigned as the loss of CO from m/z 497. Path C depicts another cross-ring cleavage resulting in a loss of 90 Da, resulting in formation of the ion of m/z 556. This product ion further dissociates mainly by Path G, resulting in the same radical species at m/z 497 as proposed for Path B. Other comparatively minor pathways observed upon CAD of m/z 556 include the loss of water, which may occur in conjunction with the loss of CO (leading to the ion at m/z 510), the loss of formaldehyde, and the loss of 72 Da. The loss of formaldehyde from m/z 556 is followed by the loss of HCO· radical, also resulting in the radical product ion at m/z 497. Paths B and C are the most prevalent fragmentation pathways for the C-bonded flavonoids studied. Path D represents a simple loss of water, mostly likely from the sugar. This dehydration reaction is followed by yet another loss of water or even loss of two water molecules. The identities of the hydroxyl groups that are lost as water molecule can't be determined with certainty, so the dehydrated structure shown in Scheme 2 is just one possibility.

Group Ib differentiation: Rhoifolin and Isorhoifolin (MW 578). Both the [Co(II) (L-H) bpy]$^+$ complexes of rhoifolin and isorhoifolin (Figure 7a and b) undergo the same major loss of the disaccharide (loss of 308 Da) as was observed upon CAD of the deprotonated species (Figure 3a and b). However, the loss of Rha (−146 Da) is also observed for both isomers, and this fragmentation pathway was not observed for the deprotonated species. In addition to these two pathways, rhoifolin also undergoes the elimination of aglycone in conjunction with the loss of Glu (relative intensity 11%), leading to the unique fragment ion at m/z 376. Apparently the 1 → 6 linkage of the rutinoside on isorhoifolin disrupts this fragmentation pathway. Note that both rhoifolin

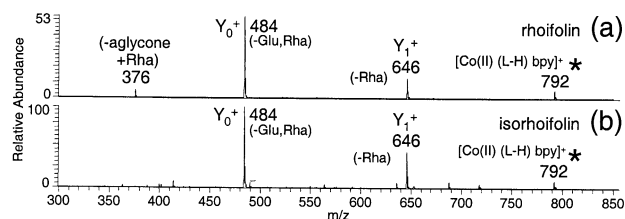**Figure 7**. CAD spectra of parent [Co(II) (L-H) bpy]$^+$ complexes of Group Ib flavonoids. The parent ions are labeled with asterisks.
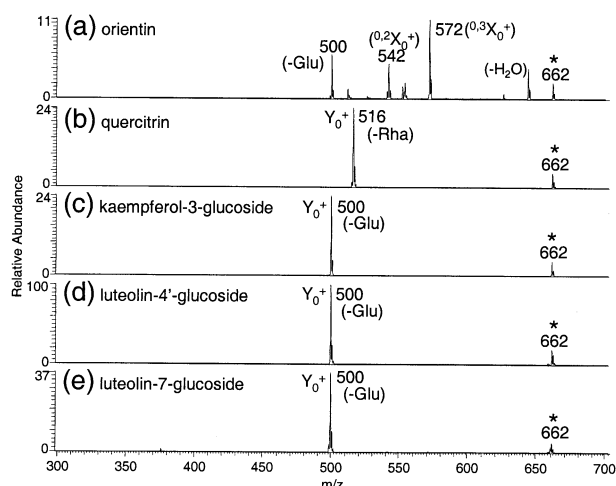
Figure 8. CAD spectra of [Co(II) (L-H) bpy]$^+$ complexes of Group II flavonoids. The parent ions are labeled with asterisks.

and apigenin-7-glucoside, both with sugars at the 7 position like isorhoifolin, undergo this loss of the aglycone. This suggests that the loss of aglycone is indicative of a sugar at the 7 position or a 1 → 2 disaccharide. The appearance of the unique ion at m/z 376 is a promising diagnostic ion for differentiation of isorhoifolin and rhoifolin, but an increase in the relative intensity of this key ion, which would be desirable,

could not be obtained for the [Co(II) (L-H) bpy]$^+$ complexes.

Group II differentiation (MW 448). The CAD spectra for the Group II [Co(II) (L-H) bpy]$^+$ complexes are shown in Figure 8, and the MS^3 data is tabulated in Table 4. The CAD spectrum of the [Co(II) (L-H) bpy]$^+$ complex of orientin was the most interesting of the five Group II isomers, with cross-ring cleavages corresponding to both Paths B and C (leading to the ions at m/z 542 and 572), in addition to loss of the entire sugar (Path A, formation of m/z 500). This isomer is clearly differentiated based on these cross-ring cleavages (Figure 8a). In addition, the [Co(II) (L-H) bpy]$^+$ complex of quercitrin is easily differentiated from the others because of its loss of Rha, resulting in the Y_0^+ complex at m/z 516 (Figure 8b), similar to what was observed for the deprotonated flavonoid. The remaining three isomers, the O-glucosides, each dissociate by loss of their terminal sugars, resulting in Y_0^+ complexes at m/z 500 (Figure 8c, d, and e), again like what was observed for the deprotonated isomers. These isomers are not differentiated via their MS^3 spectra either (Table 4). For example, isolation and CAD of the major primary fragment ion at m/z 500 for each isomer results in a dominant apparent loss of 120 Da which is the elimination of 2,2'-bipyridine and addition of two molecules of water (Scheme **1**, Path E), and the apparent loss of 138 Da

Table 4. MS^n spectra of Group II [Co(II) (L-H) bpy]$^+$ complexes

	m/z	MS/MS[a]			MS/MS/MS[a]		
		m/z	Loss	%	*m/z*	Loss	%
Orientin	662	572	90	100			
		500	162	60			
		542	120	45			
		644	18	40			
		541	121	10			
		528	134	15			
Quercitrin	662	516	146	100			
Kaempferol-3-glucoside	662	500	162	100	380	120	100
					233	267	13
					247	253	11
					472	28	8
					362	138	8
					308	192	7
					442	58	5
Luteolin-4'-glucoside	662	500	162	100	380	120	100
					362	138	12
					472	28	5
					394	106	5
Luteolin-7-glucoside	662	500	162	100	380	120	100
					233	267	34
					247	253	23
					362	138	11
					472	28	5
					394	106	5
					443	57	3

[a]MS/MS and MS/MS/MS data correspond to their parent ions (labeled *m/z*) on the left. The standard deviations of the fragment ion intensities are typically ±5%.
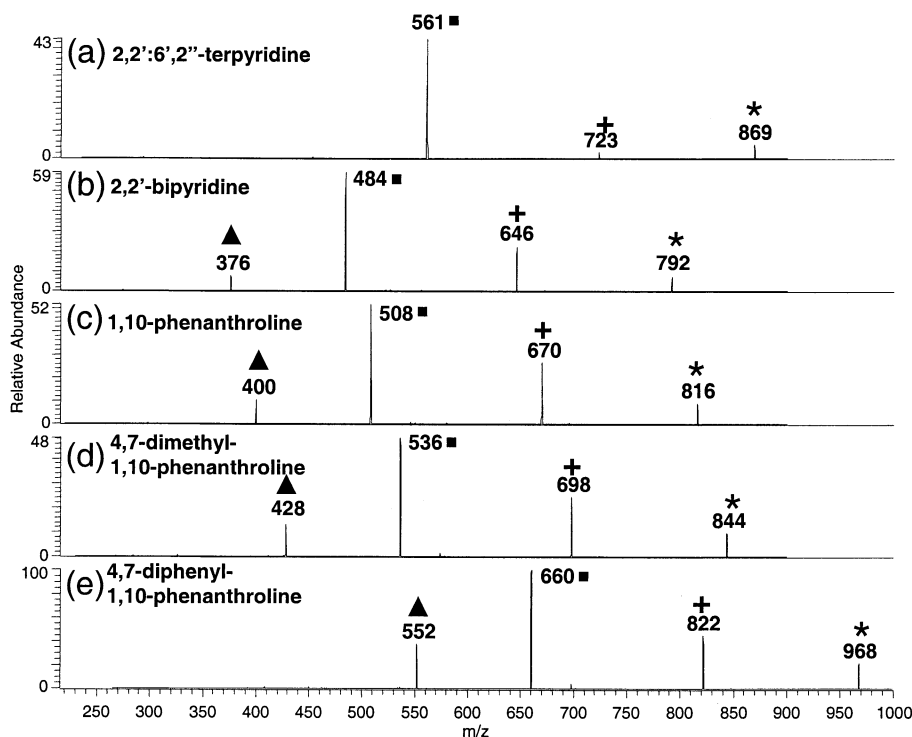
Figure 9. CAD mass spectra of [Co(II) (rhoifolin-H) pyridyl ligand]$^+$ complexes, showing relative intensities of the losses of aglycone and Rha with the variation of auxiliary ligand. The parent ion is designated with an asterisk, the loss of Rha is designated by a plus sign, the loss of disaccharide is designated by a solid square, and the loss of the aglycone and Rha is designated by a solid triangle.

which is the elimination of 2,2'-bipyridine and addition of one molecule of water. In addition, there are ions at m/z 233 and 247 which are non-specific complexes of 2,2'-bipyridine and cobalt with water or methanol, respectively. The inability to differentiate the two luteolin-glucoside isomers remained a persistent problem, and prompted us to consider the examination of other metal complexes.

Complexation with Cobalt and 4,7-Diphenyl-1,10-Phenanthroline

Based on the improvements in isomer differentiation obtained for the [Co(II) (L-H) bpy]$^+$ complexes, the use of alternative auxiliary ligands in the metal complexes was explored with the goal of increasing the "tunability" of the CAD patterns and generating more distinctive fragmentation patterns for each set of isomers, particularly for rhoifolin and isorhoifolin in Group Ib and the three undifferentiated isomers in Group II (kaempferol-3-glucoside, luteolin-4'-glucoside, and luteolin-7-glucoside). The various auxiliary ligands were assessed based on the overall signal intensity of the metal complexes and the number and intensity of the diagnostic fragment ions observed in the CAD mass spectra. The following ligands were evaluated in comparison to the results obtained for the 2,2,'-bipyridine complexes: 2,2':6',2"-terpyridine, 1,10-phenanthroline,

4,4'-dimethyl-2,2'-bipyridine and 4,7-diphenyl-1,10-phenanthroline. These ligands were selected because they retain the chelating ability attributed to the 2,2'-bipyridine skeleton, but their metal affinities are altered by the electron-releasing alkyl groups appended remote from the nitrogen atoms [77]. An example of the series of CAD mass spectra obtained by varying the auxiliary ligand is shown in Figure 9 for rhoifolin with cobalt. For the spectra shown in Figure 9, the CAD energy was adjusted to give approximately the same level of parent ion survival, thus allowing a clear comparison of the competition among the three dominant dissociation channels for the complexes containing different auxil-
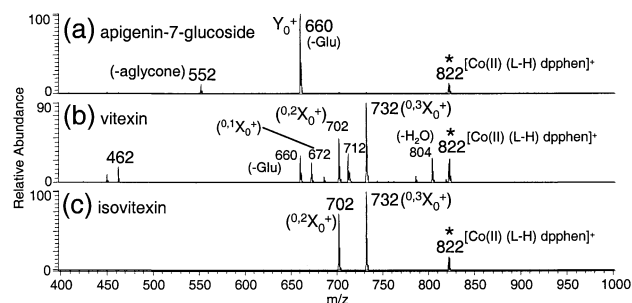

Figure 10. CAD spectra of parent [Co(II) (L-H) dpphen]$^+$ complexes of Group Ia flavonoids. The parent ions are labeled with asterisks.

Table 5. MS^n spectra of Group I [Co(II) (L-H) dpphen]$^+$ complexes

	m/z	MS/MS[a]			MS/MS/MS[a]		
		m/z	Loss	%	m/z	Loss	%
Apigenin-7-glucoside	822	660	162	100	404	256	100
					430	230	76
					632	28	41
					408	252	18
					484	176	12
					364	296	11
		552	270	12			
Vitexin	822	732	90	100	673	59	100
					714	18	34
					686	46	26
					702	30	16
					660	72	8
		702	120	56	673	29	100
					645	57	22
		712	110	36			
		660	162	35			
		804	18	30	786	18	100
					673	131	31
					744	60	21
					701	103	15
		672	50	24			
		462	360	21			
		450	372	12			
Isovitexin	822	732	90	100	673	59	100
					712	20	76
					714	18	64
					450	282	42
					686	46	38
					392	340	38
					408	324	19
					462	270	17
					424	308	13
		702	120	74	684	18	100
					673	29	94
					408	294	76
					672	30	62
					392	310	41
					645	57	22
Rhoifolin	968	660	308	100	404	256	100
					430	230	75
					632	28	40
		822	146	32	660	162	
					552	270	
		552	416	30	450	102	100
					392	160	92
					408	144	40
					462	90	28
					424	128	26
Isorhoifolin	968	660	308	100	404	256	100
					430	230	82
					632	28	45
		822	146	26	660	162	100
					552	270	12

[a]MS/MS and MS/MS/MS data correspond to their parent ions (labeled m/z) on the left. The standard deviations of the fragment ion intensities are typically ±5%.

iary ligands. The intensity of the ion due to the consecutive losses of aglycone and Glu increased ongoing from the complexes containing 2,2':6,2"-terpyridine to 4,7-diphenyl-1,10-phenanthroline, corresponding with the increasing binding energy of the pyridyl ligand to cobalt in the gas phase as determined previously by energy-variable CAD [77]. Based on a comparative assessment, 4,7-diphenyl-1,10-phenanthroline (dpphen)
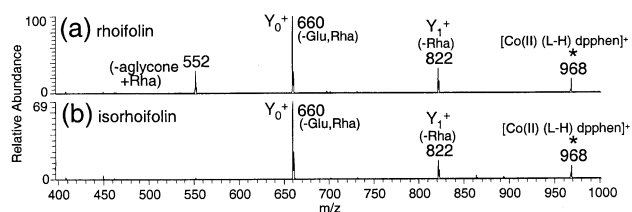
Figure 11. CAD spectra of parent [Co(II) (L-H) dpphen]$^+$ complexes of Group Ib flavonoids. The parent ions are labeled with asterisks.

resulted in metal complexes that gave the most distinctive CAD patterns, so it was used for the remainder of the study. In general, the types of fragment ions observed upon dissociation of the [Co(II) (L-H) dpphen]$^+$ complexes are the same as those already observed and rationalized for the [Co(II) (L-H) bpy]$^+$ complexes. However, the intensities of some of the key diagnostic ions which allow differentiation of isomers are increased for the [Co(II) (L-H) dpphen]$^+$ complexes, and a few new diagnostic ions are also observed upon CAD.

Group Ia differentiation: Vitexin, Isovitexin, and Apigenin-7-Glucoside (MW 432). The CAD mass spectra of the Group Ia complexes [Co(II) (L-H) dpphen]$^+$ are shown in Figure 10, and the MS^n results are summarized in Table 5. As noted for the [Co^{2+}(L-H) bpy]$^+$ complex, the CAD spectrum for the [Co(II) (L-H) dpphen]$^+$ complex of apigenin-7-glucoside complex contains only one major ion (Y$_0^+$ complex) due to the loss of the Glu (Figure 10a), but the ion due to the subsequent loss of the aglycone (m/z 552) is more intense for this complex (12% for the dpphen complex versus 4% for the bpy complex, Figure 6a versus 10a). The CAD pattern of the [Co(II) (L-H) dpphen]$^+$ complex of isovitexin is virtually the same as the one observed above for the analogous [Co(II) (L-H) bpy]$^+$ complex. The CAD spectrum of the [Co(II) (vitexin-H) dpphen] complex also contains two

additional non-specific product ions (m/z 450 and 462, Figure 10b), which are dpphen-containing ions and not diagnostic for vitexin.

Group Ib Differentiation: Rhoifolin and Isorhoifolin (MW 578) The major fragmentation pathways seen in the CAD mass spectra of the [Co(II) (L-H) dpphen]$^+$ complexes of rhoifolin and isorhoifolin (Figure 11a and b) are the same as those observed above for the analogous [Co^{2+} (L-H) bpy]$^+$ complexes (Figure 7a and b). However, the key diagnostic ion for identifying rhoifolin (i.e., the pathway due to loss of the aglycone and Glu moieties, m/z 552) is significantly more pronounced for the [Co(II) (L-H) dpphen]$^+$ complex (30% relative intensity for the dpphen complexes versus 10% relative intensity for the corresponding bpy complex, m/z 376). This subtle but important change in the CAD mass spectrum is a good demonstration of the ability to tune the fragmentation patterns and enhance the differentiation of isomers by modifying the metal affinity of the auxiliary ligand. A relatively small difference in the metal affinity of the auxiliary ligand alters the energetics for dissociation of the complex, thus changing both the accessibility of and competition among different fragmentation channels.

Group II differentiation (MW 448). Shown in Figure 12 are the CAD mass spectra of the [Co(II) (L-H) dpphen]$^+$ complexes of the Group II isomers. The CAD mass spectra of the [Co(II) (L-H) dpphen]$^+$ complexes of the Group II flavonoids are generally similar to those observed and rationalized above for the [Co(II) (L-H) bpy]$^+$ complexes (Figure 8), with a few exceptions. For example, the fragmentation pattern of the orientin complex (Figure 12a) has one extra diagnostic ion (loss of 110 Da, m/z 728). Also, the luteolin-7-glucoside isomer is now differentiated from luteolin-4'-glucoside by a new fragment ion stemming from the loss of the aglycone with the loss of the terminal sugar, resulting in the fragment ion at m/z 552 with 10% relative intensity (Figure 12e).

While kaempferol-3-glucoside and luteolin-4'-glucoside were better differentiated in the negative ion mode (Figure 4), luteolin-7-glucoside was only differentiated by using metal complexation. To differentiate kaempferol-3-glucoside and luteolin-4'-glucoside, the pair of isomers that remained the most resistant to mass spectral differentiation using metal comlexation, MS^3 experiments were performed. In the MS/MS/MS spectra obtained for the [Co(II) (L-H) dpphen]$^+$ complexes based on isolation and activation of the primary fragment ion (m/z 676, loss of the sugar, 162 Da), there are now numerous secondary fragment ions which uniquely differentiate kaempferol-3-glucoside from luteolin-4'-glucoside. These three isomers are a good example of how metal complexation may be used in conjunction with the negative ion mode for complete isomer differentiation. The MS^n data for the complexes
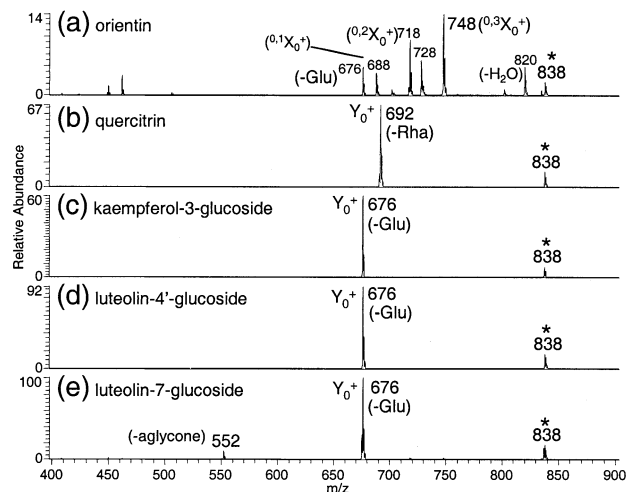

Figure 12. CAD spectra of parent [Co(II) (L-H) dpphen]$^+$ complexes of Group II flavonoids. The parent ions are labeled with asterisks.

Table 6.   MS^n Spectra of Group II [Co(II) (L-H) dpphen]$^+$ complexes

		MS/MS[a]			MS/MS/MS[a]		
	m/z	*m/z*	Loss	%	*m/z*	Loss	%
Orietin	838	748	90	100			
		718	120	71			
		728	110	46			
		820	18	36			
		676	162	32			
		688	150	29			
		462	376	25			
		450	388	11			
Quercitrin	838	692	146	100			
Kaempferol-3-glucoside	838	676	162	100	408	268	100
					423	253	48
					484	192	28
					648	28	19
					404	272	18
					496	180	13
					632	44	9
					392	284	9
					333	343	5
Luteolin-4'-glucoside	838	676	162	100	404	272	100
					430	246	67
					648	28	53
					408	268	30
					658	18	30
					647	27	27
					630	46	20
					620	56	13
					392	284	12
					442	234	12
					500	176	10
					524	152	7
Luteolin-7-glucoside	838	676	162	100	408	268	100
					423	253	51
					404	272	14
					619	57	10
					430	246	10
		675	163	30			
		552	286	11			

[a]MS/MS and MS/MS/MS data correspond to their parent ions (labeled *m/z* on the left). The standard deviations of the fragment ion intensities are typically ±5%.

of the Group II isomers with Co/dpphen is tabulated in Table 6.

Position of glycosylation.   Since complexation with cobalt and dpphen resulted in the most interesting fragmentation patterns in this study, it is worthwhile to compare the general types of diagnostic ions observed as a function of the positions of glycosylation for the various flavonoids. For example, it is interesting to note that for C-bonded isomers (vitexin, isovitexin, orientin), the $^{0,1}X_0^+$ is only observed for those flavonoids glycosylated at the 8-position as with vitexin and orientin (Figures 10b and 12a, respectively), but not for glycosylation at the 6-position as in the isovitexin isomer (Figure 10c). For the 7–O-bonded glucosides (apigenin-7-glucoside, rhoifolin, isorhoifolin, luteolin-7-glucoside), the loss of the aglycone or the aglycone and terminal sugar is always observed (Figures 10a, 11a,

and 12e) except for the rutinosides. The lack of this pathway for 7–O-bonded rutinoside isorhoifolin (Figure 11b) is likely related to the site of metal complexation and/or conformation of the disaccharide when coordinated to the metal ion. These general trends in the diagnostic ions observed with the position of glycosylation are an extremely useful feature of metal complexation for structural determination of flavonoids.

Conclusions

Metal complexation with an auxiliary ligand has been used to differentiate flavonoid glycoside isomers by ESI-tandem mass spectrometry. In the presence of a metal and an appropriate auxiliary ligand, complexes of the type [Co(II) (flavonoid-H) ligand]$^+$ are formed

which are generally one to two orders of magnitude greater in intensity than the intensities of the molecular ions observed in positive or negative ionization modes, thereby improving limits of detection. CAD of the metal complexes results in fragmentation patterns which are often different that those of the protonated or deprotonated species and may be used separately or in conjunction with these modes for isomer differentiation. This general metal complexation technique has been improved with the use of 4,7-diphenyl-1,10-phenanthroline as a new auxiliary chelating ligand. In particular, the differentiation of disaccharide isomers with $1 \rightarrow 2$ and $1 \rightarrow 6$ linkages and the two luteolin-glucoside isomers is now possible based on formation and detection of unique fragment ions for each isomer.

Acknowledgments

References

1. Pietta, P. Flavonoids in Medicinal Plants. *Flavonoids in Health and Disease;* In: Rice-Evans, C. A.; Packer, L., Eds.; Marcel Dekker: New York, 1998; p 62.
2. Berhow, C. A.; Vaughn, S. F. Higher Plants Flavonoids: Biosynthesis and Chemical Ecology. In *Principles and Practices in Plant Ecology, Allochemical Interactions*; CRC Press: Boca Raton, FL, 1999; pp 423-437.
3. Lin, Y. Y.; Ng, K. J.; Yang, S. Characterization of Flavonoids by Liquid Chromatography-Tandem Mass Spectrometry. *J. Chromatogr.* **1993,** *629,* 389–393.
4. Morand, C.; Crespy, V.; Manach, C.; Besson, C.; Demigne, C.; Remesy, C. Plasma Metabolites of Quercetin and their Antioxidant Properties. *Am. J. Physiol.* **1998,** *275,* R212–R219.
5. Rice-Evans, C. A.; Miller, N. J. Antioxidant Activities of Flavonoids as Bioactive Components of Food. *Biochem. Soc. Trans.* **1996,** *24,* 790–795.
6. Pratt, D. E. *Natural Antioxidants from Plant Material*; ACS Symp. Ser. No. 507, 1992; pp 54–71.
7. Dixon, R. A.; Steele, C. L. Flavonoids and Isoflavonoids—A Gold Mine for Metabolic Engineering. *Trends Plant Sci.* **1999,** *4,* 394–400.
8. Hertog, M. G. ; Kromhout, D.; Aravanis, C.; Blackburn, H.; Buzina, R.; Fidanza, F.; Giampaoli, S.; Jansen, A.; Menotti, A.; Nedeljkovic, S.; Pekkarinen, M.; Simic, B. S.; Toshima, H.; Feskens, E. J. M.; Hollman, P. C. H.; Katan, M. B. Flavonoid Intake and Long-Term Rish of Coronary Heart Disease and Cancer in the Seven Countries Study. *Arch. Intern. Med.* **1995,** *155,* 381–386.
9. Hertog, M. G.; Feskens, E. J. M.; Hollman, P. C. H.; Katan, M. B.; Kromhout, D. Dietary Antioxidant Flavonoids and Risk of Coronary Heart Disease: the Zutphen Elderly Study. *Lancet* **1993,** *342,* 1007–1011.
10. Knekt, P.; Jarvinen, R.; Reunanen, A.; Maatela, J. Flavonoid Intake and Coronary Mortality in Finland: A Cohort Study. *Br. Med. J.* **1996,** *312,* 478–481.
11. Bors, W.; Heller, W.; Michel, C. The Chemistry of Flavonoids. *Flavonoids in Health and Disease;* In: Rice-Evans, C. A.; Packer, L., Eds.; Marcel Dekker: New York, 1998; pp 111–136.
12. Stobiecki, M. Application of Mass Spectrometry for Identification and Structural Studies of Flavonoid Glycosides. *Phytochemistry* **2000,** *54,* 237–256.
13. Mabry, T. J.; Markham, K. R. Mass Spectrometry of Flavonoids. *The Flavonoids;* In: Harborne, J. B.; Mabry, T. J.; Mabry, H., Eds.; Academic Press: New York, 1975; pp 79–126.
14. Besson, E.; Besset, A.; Bouillant, M.-L.; Chopin, J.; van Brederode, J.; van Nigtevecht, G. Genetically Controlled 2 ≫-O-Glycosylation of Isovitexin in the Petals of *Melandrium album.* *Phytochemistry* **1979,** *18,* 657–658.
15. Bouillant, M.-L.; Ferreres de Arce, F.; Favre-Bonvin, J.; Chopin, J.; Zoll, A.; Mathieu, G. Structural Determination of 6-C-Diglycosylflavones and 6-C-Dlycosyl-8-C-Diglycosylflavones by Mass Spectrometry of Their Permethyl Ethers. *Phytochemistry* **1984,** *23,* 2653–2657.
16. Sakushima, A.; Nishibe, S. Taxifolin 3-Arabinoside from *Trachelospermum jasminoides* var. Pubescens. *Phytochemistry* **1988,** *27,* 948–950.
17. Schels, H.; Zinsmeister, H. D.; Pfleger, K. Mass Spectrometry of Silylated Flavone and Flavanone Glycosides. *Phytochemistry* **1978,** *17,* 523–526.
18. Becchi, M.; Fraisse, D. Fast Atom Bombardment and Fast Atom Bombardment Collision Activated Dissociation/Mass-Analysed Ion Kinetic Energy Analysis of C-Glycosidic Flavonoids. *Biomed. Environm. Mass Spectrom.* **1989,** *18,* 122–130.
19. Bridle, P.; Loeffler, R. S. T.; Timberlake, C. F.; Self, R. Cyanidin 3-Malonylglucoside in *Cychorium intybus.* *Phytochemistry* **1984,** *23,* 2968–2969.
20. Claeys, M.; Li, Q.; Van den Heuvel, H.; Dillen, L. Mass Spectrometric Studies on Flavonoid Glycosides. *Applications of Modern Mass Spectrometry in Plant Sciences*; Newton, R. P.; Walton, T. J., Eds.; Clarendon Press: Oxford, 1996; pp 182–194.
21. Crow, F. C.; Tomer, K. B.; Looker, J. H.; Gross, M. L. Fast Atom Bombardment and Tandem Mass Spectrometry for Structure Determination of Steroid and Flavonoid Glycosides. *Anal. Biochem.* **1986,** *155,* 286–297.
22. Domon, B.; Hostettmann, K. Mass Spectrometric Studies of Underivitized Polyphenolic Glycosides. *Phytochemistry* **1985,** *24,* 575–580.
23. Li, Q. M.; van den Heuvel, H.; Dillen, L.; Claeys, M. Differentiation of 6-C- and 8-C-Glycosidic Flavonoids by Positive Ion Fast Atom Bombardment and Tandem Mass Spectrometry. *Biol. Mass Spectrom.* **1992,** *21,* 213–221.
24. Li, Q. M.; Claeys, M. Characterization and Differentiation of Diglycosyl Flavonoids by Positive Fast Atom Bombardment and Tandem Mass Spectrometry. *Biol. Mass Spectrom.* **1994,** *23,* 406–416.
25. Saito, N.; Abe, K.; Honda, R.; Timberlake, C. F.; Bridle, P. Acylated Delphinidin Glucosides and Flavonols from *Clitoria ternatea.* *Phytochemistry* **1985,** *24,* 1583–1586.
26. Sakushima, A.; Nishibe, S.; Takeda, T.; Ogihara, Y. Positive and Negative Ion Mass Spectra of Flavonoid Glycosides by Fast Atom Bombardment. *Mass Spectrosc.* **1988,** *36(71),* 80.
27. Sakushima, A.; Nishibe, S. Mass Spectrometry in the Structural Determination of Flavonol Triglycosides from *Vinca major.* *Phytochemistry* **1988,** *27,* 915–919.
28. Stobiecki, M.; Olechnowicz-Stepien, W.; Rzadkowska-Bodalska, H.; Cisowski, W.; Budko, E. Identification of Flavonoid Glycosides Isolated from Plants by Fast Atom Bombardment Mass Spectrometry and Gas Chromatography/Mass Spectrometry. *Biomed. Environm. Mass Spectrom.* **1988,** *15,* 589–594.
29. Sumner, L. W.; Paiva, N. L.; Dixon, R. A.; Geno, P. W. High Performance Liquid Chromatography/Continuous-Flow Liquid Secondary Mass Spectrometry of Flavonoid Glycosides in Leguminous Plant Extracts. *J. Mass Spectrom.* **1996,** *31,* 472–485.

30. Wolfender, J.-L.; Maillard, M.; Marston, A.; Hostettmann, K. Mass Spectrometry of Underivatized Naturally Occuring Glycosides. *Phytochem. Anal.* **1992,** *3,* 193–214.

31. Ma, Y. L.; Li, Q. M.; Van den Heuvel, H.; Claeys, M. Characterization of Flavone and Flavonol Aglycones by Collision-induced Dissociation Tandem Mass Spectrometry. *Rapid Commun. Mass Spectrom.* **1997,** *11,* 1357–1364.

32. Cuyckens, F.; Shahat, A. A.; Pieters, L.; Claeys, M. Direct Stereochemical Assignment of Hexose and Pentose Residues in Flavonoid O-glycosides by Fast Atom Bombardment and Electrospray Ionization Mass Spectrometry. *J. Mass Spectrom.* **2002,** *37,* 1272–1279.

33. Ma, Y.-L.; Cuyckens, F.; Van den Heuvel, H.; Claeys, M. Mass Spectrometric Methods for the Characterization and Differentiation of Isomeric O-diglycosyl Flavonoids. *Phytochem. Anal.* **2001,** *12,* 159–165.

34. Ma, Y. L; Van den Heuvel, H.; Claeys, M. Characterization of 3-Methoxyflavones Using Fast-Atom Bombardment and Collision-Induced Dissociation Tandem Mass Spectrometry. *Rapid Commun. Mass Spectrom.* **1999,** *13,* 1932–1942.

35. Ma, Y.-L.; Vedernikova, I.; Van den Heuvel, H.; Claeys, M. Internal Glucose Residue Loss in Protonated O-Diglycosyl Flavonoids upon Low-Energy Collision-Induced Dissociation. *J. Am. Soc. Mass Spectrom.* **2000,** *11,* 136–144.

36. Hughes, R. J.; Croley, T. R.; Metcalfe, C. D.; March, R. E. A Tendem Mass Spectrometric Study of Selected Characteristic Flavonoids. *Int. J. Mass Spectrom.* **2001,** *210/211,* 371–385.

37. Brolis, M.; Gabetta, B.; Fuzzati, N.; Pace, R.; Panzeri, F.; Peterlongo, F. Identification by High-Performance Liquid Chromatography-Diode Array Detection-Mass Spectrometry and Quantification by High-Performance Liquid Chromatography-UV Absorbance Detection of Active Constituents of *Hypericum perforarum.* *J. Chromatogr. A* **1998,** *825,* 9–16.

38. Pietta, P.; Facino, R. M.; Carini, M.; Mauri, P. Thermospray Liquid Chromatography-Mass Spectrometry of Flavonol Glycosides from Medicinal Plants. *J. Chromatogr. A* **1994,** *661,* 121–126.

39. Iida, J.; Murata, R. Application of Thermospray Liquid Chromatography/Mass Spectrometry to Analysis of Glycosides. *Anal. Sci.* **1991,** *7,* 963–966.

40. Grayer, R. J.; Kite, G. C.; Abou-Zaid, M.; Archer, L. J. The Application of Atmospheric Ionisation Liquid Chromatography-Mass Spectrometry in the Chemotaxonomic Study of Flavonoids: Characterization of Flavonoids from *Ocimum gratissimum* var. gratissimum. *Phytochem. Anal.* **2000,** *11,* 257–267.

41. Jensen, A. G.; Ndjoko, K.; Wolfender, J.-L.; Hostettmann, K.; Camponovo, F.; Soldati, F. Liquid Chromatography-Atmospheric Pressure Chemical Ionization/Mass Spectrometry: A Rapid and Selective Method for the Quantitative Determination of Ginkgolides and Bilobalide in Ginkgo Leaf Extracts and Phytopharmaceuticals. *Phytochem. Anal.* **2002,** *13,* 31–38.

42. Krishnan, H. B. Identification of Genistein, an Anticarcinogenic Compound, in the Edible Tubers of the American Groundnut *Apios Americana* Medikus. *Crop Sci.* **1998,** *38,* 1052–1056.

43. Barnes, K. A.; Smith, R. A.; Williams, K.; Damant, A. P.; Shepherd, M. J. A Microbore High Performance Liquid Chromatography/Electrospray Ionization Mass Spectrometry Method for the Determination of the Phytoestrogens Genistein and Daidzein in Comminuted Baby Foods and Soya Flour. *Rapid Commun. Mass Spectrom.* **1998,** *12,* 130–138.

44. Poon, G. K. Analysis of Catechins in Tea Extracts by Liquid Chromatography-Electrospray Ionization Mass Spectrometry. *J. Chromatogr. A* **1998,** *794,* 63–74.

45. Fabre, N.; Rustan, I.; de Hoffmann, E.; Quetin-Leclercq, J. Determination of Flavone, Flavonol, and Flavanone Algycones by Negative Ion Liquid Chromatography Electrospray Ion Trap Mass Spectrometry. *J. Am. Soc. Mass Spectrom* **2001,** *12,* 707–715.

46. Raffaelli, A.; Moneti, G.; Mercati, V.; Toja, E. Mass Spectrometric Characterization of Flavonoids in Extracts from *Passiflora incarnata.* *J. Chromatogr. A* **1997,** *777,* 223–231.

47. Stevens, J. F.; Taylor, A. W.; Deinzer, M. L. Quantitative Analysis of Xanthohumol and Related Prenylflavonoids in Hops and Beer by Liquid Chromatography-Tandem Mass Spectrometry. *J. Chromatogr. A* **1999,** *832,* 97–107.

48. Hakkinen, S. H.; Karenlamp, S. O.; Herinonen, I. M.; Mykkanen, H. M.; Torronen, A. R. Content of the Flavonols Quercetin, Myricetin, and Kaempferol in 25 Edible Berries. *J. Agric. Food Chem.* **1999,** *47,* 2274–2279.

49. Satterfield, M.; Black, D. M.; Brodbelt, J. S. Detection of the Isoflavone Aglycones Genistein and Daidzein in Urine Using Solid-Phase Microextraction-High-Performance Liquid Chromatography-Electrospray Ionization Mass Spectrometry. *J. Chromatogr. B* **2001,** *759,* 33–41.

50. Cuyckens, F.; Rozenburg, R.; Hoffmann, E.; Claeys, M. Structure Characterization of Flavonoid O-diglycosides by Positive and Negative Nano-Electrospray Ionization Ion Trap Mass Spectrometry. *J. Mass Spectrom.* **2001,** *36,* 1203–1210.

51. Waridel, P.; Wolfender, J.-L.; Ndjoko, K.; Hobby, K. R.; Major, H. J.; Hostettmann, K. Evaluation of Quadrupole Time-of-Flight Tandem Mass Spectrometry and Ion-trap Multiple-Stage Mass Spectrometry for the Differentiation of C-glycosidic Flavonoid Isomers. *J. Chromatogr. A* **2001,** *926,* 29–41.

52. Hvattum, E.; Ekeberg, D. Study of the Collision-Induced Radical Cleavage of Flavonoid Glycosides Using Negative Electrospray Ionization Tandem Quadrupole Mass Spectrometry. *J. Mass Spectrom.* **2003,** *38,* 43–49.

53. Alvarez, E.; Vartanian, V.; Brodbelt, J. S. Metal Complexation Reactions of Quinolone Antibiotics in a Quadrupole Ion Trap. *Anal. Chem.* **1997,** *69,* 1147–1155.

54. Alvarez, E.; Brodbelt, J. S. Evaluation of Metal Complexation as an Alternative to Protonation for Electrospray Ionization of Pharmaceutical Compounds. *J. Am. Soc. Mass Spectrom.* **1998,** *9,* 463–472.

55. Shen, J.; Brodbelt, J. S. Post-Column Metal Complexation of Quinolone Antibiotics in a Quadrupole Ion Trap. *Rapid Comm. Mass Spectrom.* **1999,** *13,* 1381–1389.

56. Satterfield, M.; Brodbelt, J. S. Enhanced Detection of Flavonoids by Metal Complexation and Electrospray Ionization Mass Spectrometry. *Anal. Chem.* **2000,** *72,* 5898–5906.

57. Satterfield, M.; Brodbelt, J. S. Structural Characterization of Flavonoids Glycosides by Collisionally Activated Dissociation of Metal Complexes. *J. Am. Soc. Mass Spectrom.* **2001,** *12,* 537–549.

58. Zhang, J.; Brodbelt, J. S. Structural Characterization and Isomer Differentiation of Chalcones by Electrospray Ionization Tandem Mass Spectrometry. *J. Mass Spectrom.* **2003,** *38,* 555–572.

59. Mateos, R.; Espartero, J. L.; Trujillo, M.; Rios, J. J.; Leon-Camacho, M.; Alcudia, F.; Cert, A. Determination of Phenols, Flavones, and Lignans in Virgin Olive Oils by Solid-Phase Extraction and High-Performance Liquid Chromatography with Diode Array Ultraviolet Detection. *J. Agric. Food Chem.* **2001,** *49,* 2185–2192.

60. Gil-Izquierdo, A.; Gil, M. I.; Ferreres, F.; Tomas-Barberan, F. A. In Vitro Availability of Flavonoids and Other Phenolics in Orange Juice. *J. Agric. Food Chem.* **2001,** *49,* 1035–1041.

61. Trichopoulou, A.; Vasilopoulou, E.; Hollman, P.; Chamalides, C.; Foufa, E.; Kaloudis, T.; Kromhout, D.; Miskaki, P.; Petrochilou, I.; Poulima, E.; Stafilakis, K.; Theophilou, D. Nutritional Composition and Flavonoid Content of Edible Wild Greens and Green Pies: A Potential Rich Source of Antioxidant Nutrients in the Mediterranean Diet. *Food Chem.* **2000,** *70,* 319–323.

62. Miean, K.; Mohamed, S. Flavonoid (Myricetin, Quercetin, Kaempferol, Luteolin, and Apigenin) Content of Edible Tropical Plants. *J. Agric. Food Chem.* **2001,** *49,* 3106–3112.

63. Bilyk, A.; Sapers, G. M. Distribution of Quercetin and Kaempferol in Lettuce, Kale, Chive, Garlic Chive, Leek, Horseradish, Red Radish, and Red Cabbage Tissues. *J. Agric. Food Chem.* **1985,** *33,* 226–228.

64. Price, K. R.; Colquhoun, I. J.; Barnes, K. A.; Rhodes, M. J. C. Composition and Content of Flavonol Glycosides in Green Beans and Their Fate During Processing. *J. Agric. Food Chem.* **1998,** *46,* 4898–4903.

65. Karadeniz, F.; Durst, R.; Wrolstad, R. Polyphenolic Composition of Raisins. *J. Agric. Food Chem.* **2000,** *48,* 5343–5350.

66. Hertog, M.; Hollman, P.; Venema, D. Optimization of a Quantitative HPLC Determination of Potentially Anticarcinogenic Flavonoids in Vegetables and Fruits. *J. Agric. Food Chem.* **1992,** *40,* 1591–1598.

67. Domon, B.; Costello, C. E. A Systematic Nomenclature for Carbohydrate Fragmentations in FAB-MS/MS Spectra of Glycoconjugates. *Glycoconj. J.* **1988,** *5,* 397–409.

68. Quemener, B.; Desire, C.; Debrauwer, L.; Rathahao, E. Structural Characterization of Both Positive and Negative Electrospray Ion Trap Mass Spectrometry of Oligogalacturonates Purified by High-Performance Anion-Exchange Chromatography. *J. Chromatogr. A.* **2003,** *984,* 185–194.

69. Pfenninger, A.; Karas, M.; Finke, B.; Stahl, B. Structural Analysis of Underivatized Neutral Human Milk Oligosaccharides in the Negative Ion Mode by Nanoelectrospray MS^n. *J. Am. Soc. Mass Spectrom.* **2002,** *13,* 1331–1340.

70. Sheeley, D. M.; Reinhod, V. N. Structural Characterization of Carbohydrates Sequence, Linkage, and Branching in a Quadrupole Ion Trap Mass Spectrometer: Neutral Oligosaccharides and N-Linked Glycans. *Anal. Chem.* **1998,** *70,* 3053–3059.

71. Salpin, J.-Y.; Tortajada, J. Structural Characterization of Hexoses and Pentoses Using Lead Cationization. An Electrospray Ionization and Tandem Mass Spectrometric Study. *J. Mass Spectrom.* **2002,** *37,* 379–388.

72. Reid, G. E.; O'Hair, A. J.; Styles, M. L.; McFadyen, W. D.; Simpson, R. J. Gas Phase Ion-Molecule Reactions in a Modified Ion Trap: H/D Exchange of Noncovalent Complexes and Coordinatively Unsaturated Platinum Complexes. *Rapid Commun. Mass Spectrom.* **1998,** *12,* 1701–1708.

73. Vachet, R. W.; Hartman, J. A. R.; Callahan, J. H. Ion-Molecule Reactions in a Quadrupole Ion Trap as a Probe of the Gas-Phase Structure of Metal Complexes. *J. Mass Spectrom.* **1998,** *33,* 1209–1225.

74. Vachet, R. W.; Hartman, J. A. R.; Gerner, J. W.; Callahan, J. H. Investigation of Metal Complex Coordination Structure Using Collision-Induced Dissociation and Ion-Molecule Reactions in a Quadrupole Ion Trap Mass Spectrometer. *Int. J. Mass Spectrom.* **2001,** *204,* 101–112.

75. Perera, B. A.; Gallardo, A. L.; Barr, J. M.; Tekarli, S. M.; Anbalagan, V.; Talaty, E. R.; Van Stipdonk, M. J. Influence of a Ring Substituent on the Tendency to form H_2O Adducts to Ag^+ Complexes with Phenylalanine Analogues in an Ion Trap Mass Spectrometer. *J. Mass Spectrom.* **2002,** *37,* 401–413.

76. Perera, B. A.; Ince, M. P.; Talaty, E. R.; Van Stipdonk, M. J. Gas Phase Attachment of Water and Methanol to Ag(I) Complexes with α-Amino Acids in an Ion Trap Mass Spectrometer. *Rapid Commun. Mass Spectrom.* **2001,** *15,* 615–622.

77. Satterfield, M.; Brodbelt, J. S. Relative Binding Energies of Gas-Phase Pyridyl Ligand/Metal Complexes by Energy-Variable Collisionally Activated Dissociation in a Quadrupole Ion Trap. *Inorg. Chem.* **2001,** *40,* 5393–5400.